Ultrasound in Med. & Biol., Vol. 45, No. 3, pp. 660−671, 2019

0301-5629/$ - see front matter

https://doi.org/10.1016/j.ultrasmedbio.2018.10.012

● *Original Contribution*

THE VALUE OF PERCUTANEOUS SHOULDER PUNCTURE WITH CONTRAST-ENHANCED ULTRASOUND IN DIFFERENTIATION OF ROTATOR CUFF TEAR SUBTYPES: A PRELIMINARY PROSPECTIVE STUDY

YA-QUN TANG,[*,†] CHUN ZENG,[‡] XUN-TONG SU,[‡] SU-SHU LI,[*] WEN-HONG YI,[*] JING-JIAO XU,[*] GUI-QIN WU,[‡] YAN-JUN CHEN,[§] MIAN-WEN LI,[§] and HONG-MEI LIU[*]

[*] Department of Ultrasound, Guangdong Second Provincial General Hospital, Guangzhou, China; [†] Department of Ultrasound, Zhuhai Hospital Affiliated with Jinan University, Zhuhai People's Hospital, Zhuhai, China; [‡] Department of Sports Medicine and Arthroscopy, Third Affiliated Hospital of Southern Medical University, Orthopaedic Institute of Guangdong Province, Guangzhou, China; and [§] Department of Medical Imaging, Third Affiliated Hospital of Southern Medical University, Orthopaedic Institute of Guangdong Province, Guangzhou, China

(*Received* 12 *June* 2018; *revised* 11 *September* 2018; *in final from* 4 *October* 2018)

Abstract—Imaging tests perform relatively well in the detection of rotator cuff tears (RCTs), exhibiting high sensitivity and specificity, mainly among larger full-thickness tears (tear width >1 cm). However, these tests are relatively less accurate in the detection of small full-thickness tears and partial-thickness tears. The purpose of this study was to determine the feasibility of percutaneous ultrasound-guided tendon lesionography (PUTL) using the SonoVue and the value of percutaneous shoulder puncture *via* contrast-enhanced ultrasound (CEUS)—a combination of percutaneous ultrasound-guided subacromial bursography (PUSB) and PUTL—in the detection of RCT subtypes. Conventional ultrasound (US), CEUS and magnetic resonance imaging (MRI) were performed and prospectively evaluated in 97 patients who had undergone arthroscopy because of suspected RCTs. The rates of detection of the various subtypes of RCTs using CEUS, PUSB, PUTL, US and MRI were evaluated. The RCT subtype detection rate *via* CEUS was significantly higher than the rates *via* US and MRI (96.9%, 74.2% and 76.3%, respectively), as were the detection rates for small full-thickness tears combined with partial-thickness tears (98.2%, 60.0% and 61.8%, respectively). The detection rate with PUSB was significantly higher than those with US and MRI in assessing full-thickness tears combined with bursal-side partial-thickness tears (93.9%, 65.3% and 65.3%, respectively). The detection rate with PUTL was significantly higher than those with US and MRI in assessing the corresponding subtypes (100.0%, 69.2% and 76.9%, respectively). On the basis of our findings, we consider PUTL a tolerable and feasible procedure. Percutaneous shoulder puncture using CEUS can be an effective alternative method with better diagnostic performance than US and MRI for the detection of RCT subtypes. (E-mail: hongmeiliu3@163.com)

Key Words: **Rotator cuff tears, Ultrasonography, Contrast-enhanced ultrasound, Puncture, Bursography, Lesionography, Magnetic resonance imaging.**

INTRODUCTION

Shoulder pain, with a self-reported prevalence of 16%−26% in the general population (Mitchell et al. 2005), is the third most common reason for medical consultations on musculoskeletal disorders (Urwin et al. 1998). Rotator cuff tendon diseases are the most common causes of shoulder pain, especially diseases caused by wear or tear (Lenza et al. 2013). The etiologies of rotator cuff tears (RCTs) (Fig. 1) are multifactorial and have been much debated; they include hypovascularity, age-related degeneration, trauma and impingement (Brooks et al. 1992; Tashjian 2012). Awareness of the etiology is beneficial for selecting the most appropriate treatment.

Although the gold standard for the diagnosis of RCTs is arthroscopy (Franceschi et al. 2012), the majority of cases are diagnosed and managed based on clinical data and imaging tests, such as ultrasound (US) and magnetic resonance imaging (MRI). Many elderly people with degenerative RCTs are asymptomatic (Reilly et al. 2006; van Kampen et al. 2014), and the value of

Address correspondence to: Hong-Mei Liu, Department of Ultrasound, Guangdong Second Provincial General Hospital, Guangzhou 510317, China. E-mail: hongmeiliu3@163.com

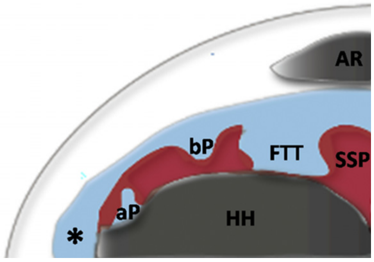

Fig. 1. Schematic of rotator cuff tear (RCT) subtypes. * = subacromial–subdeltoid bursa; aP = articular-side partial-thickness tear; AR = acromion; bP = bursal-side partial-thickness tear; FTT = full-thickness tear; HH = humeral head; SSP = supraspinatus.

physical examinations is controversial (Hanchard et al. 2013; Jain et al. 2017). Imaging tests perform relatively well in the detection of RCTs, exhibiting high sensitivity and specificity, mainly among larger full-thickness tears (tear width >1 cm). However, these tests are relatively less accurate in the detection of small full-thickness tears and partial-thickness tears (Ellman 1990; Hodler et al. 1992; Lenza et al. 2013; Rutten et al. 2010; Singisetti and Hinsche 2011).

The morbidity related to partial-thickness tears is approximately two times higher than that related to full-thickness tears (Resnick et al. 2007). Histologically, spontaneous healing of RCTs is rare (Fukuda 2000; Tashjian 2012), even after surgical repair (Massoud et al. 2002). Untreated tears may enlarge (Safran et al. 2011; Tashjian 2012), and full-thickness tears more frequently lead to fatty degeneration and atrophy of the shoulder musculature, which can increase the risk of tear recurrence after surgical repair (Gladstone et al. 2007; Kim et al. 2010). Hence, for partial-thickness and small full-thickness tears, surgery is considered a treatment option if the clinical symptoms are severe and cannot be sufficiently alleviated after conservative management (Donohue et al. 2016; Fukuda et al. 1996; Wright and Cofield 1996). Precise and timely diagnosis facilitates early optimization of the clinical management approach (Brooks et al. 1992) by directing detection and avoiding missed diagnosis during arthroscopy with information on tear size and location.

Shoulder arthrography, including direct MR arthrography and arthrosonography, carries a high rate of detection of RCTs (Chun et al. 2010; Lee et al. 2014; Meister et al. 2004; Probyn et al. 2007). It is superior for assessing full-thickness and articular partial-thickness tears and can facilitate diagnosis, whereas the misdiagnosis rates for bursal-side and intra-substance partial-thickness tears are relatively higher. A possible reason for this may be the technique mechanism, as intra-articular contrast agents can outline the undersurface of the cuff (Chun et al. 2010; González 2013). Some studies have reported that indirect MR arthrography is helpful in increasing the rates of detection of bursal-side and intra-substance partial-thickness tears (Choo et al. 2015; Yagci et al. 2001) by enhancing the highly vascular synovial membrane or the inflamed tissue within the joint cavity (Song et al. 2011; Yagci et al. 2001); however, this technique is more experience dependent (González 2013), compared with the direct technique. In general, MR techniques are intrinsically superior, but there are also some contraindications to their use. Some authors have investigated the intracavitary use of ultrasound contrast agents, such as in percutaneous ultrasound-guided subacromial bursography (PUSB) (Cheng et al. 2015), which could make up for the deficiencies of shoulder arthrography. However, Cheng et al. (2015) reported that PUSB does not evaluate articular-side partial-thickness tears effectively. Recently, Bertuglia et al. (2014) reported that contrast-enhanced ultrasound (CEUS) is an effective technique for reliably identifying the presence and depth of surgically induced intra-synovial longitudinal tears in *ex vivo* tendons.

Based on previous research, we attempted to explore two alternative percutaneous shoulder puncture techniques using CEUS—PUSB and percutaneous ultrasound-guided tendon lesionography (PUTL)—to assess RCT subtypes by evaluating tear locations and extents.

METHODS

Patients

Three hundred twenty-five consecutive patients (total of 325 shoulders) with suspected RCTs were recruited by orthopedic surgeons. The patients were referred for US and MRI of the shoulder at a general hospital between January 2014 and January 2018.

The study is prospective with a surgical correlation. The inclusion criteria for patients recommended for surgery were as follows: (i) full-thickness tears diagnosed on both US and MRI; and (ii) previous conservative treatment such as physiotherapy longer than 3 mo without sufficient symptom (shoulder pain or dysfunction) relief. Ultimately, we prospectively enrolled 98 consecutive patients who underwent US, MRI, CEUS and arthroscopy. Imaging tests performed on the same patient were all performed within 2 wk, and preliminary US and CEUS were performed on the same day. We excluded 1 patient with an intra-substance partial-thickness tear identified on CEUS but no tear identified during arthroscopy, as intra-substance partial-thickness tears could not be confirmed during shoulder arthroscopy. Accordingly, the final study population consisted of 97 patients (Fig. 2).

The ethics committee of Guangdong Second Provincial General Hospital, approved the study, and all participants provided a signed informed consent.

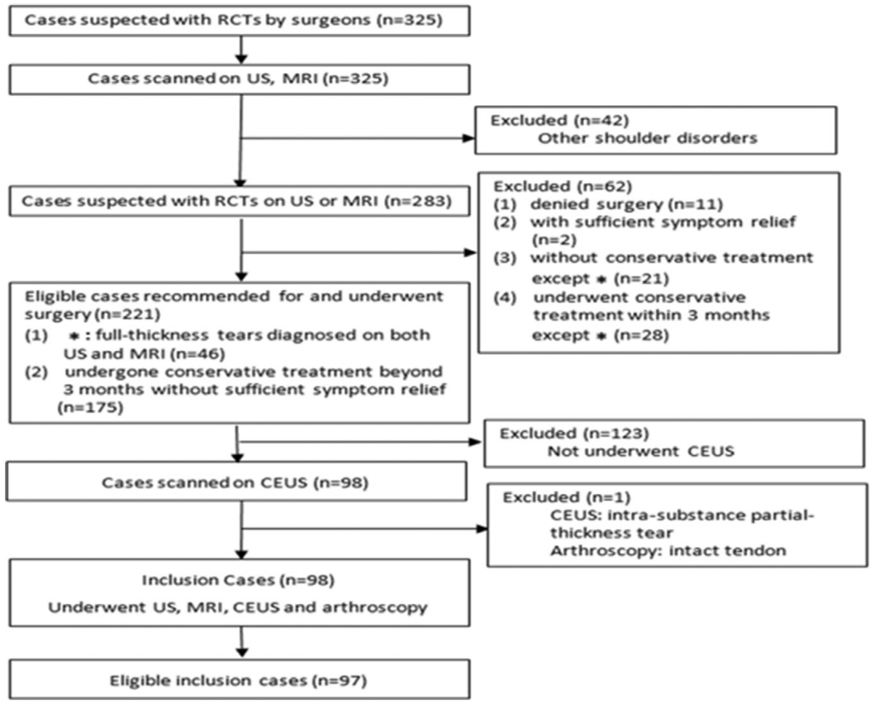

Fig. 2. Flow diagram of study population. CEUS = contrast-enhanced ultrasound; MRI = magnetic resonance imaging; RCTs = rotator cuff tears; US = ultrasound.

Ultrasonography examination and imaging analysis

Equipment and materials. The US and CEUS examinations were performed using a Logiq S8 ultrasound system (General Electric Medical Systems, Fairfield, CT, USA), equipped with contrast-tuned imaging technology. An ML6-15 matrix linear transducer was used in the US examination, and a 9 L linear transducer was used in the CEUS procedures. The mechanical index value for CEUS was 0.12.

SonoVue (Bracco, Italy) solution was used for CEUS contrast. A solution of 1.5 mL of the SonoVue solution was diluted to 15 mL with 13.5 mL of 0.9% sodium chloride. A solution of 2% lidocaine was used as an anesthetic during the CEUS procedure.

Procedure. Sonographic evaluation of the rotator cuff was performed according to the technical guidelines for shoulder ultrasound as recommended by the European Society of Skeletal Radiology (Daenen et al. 2007). We scanned the patients in both the Crass and modified Crass positions, as tolerated, to better evaluate the supraspinatus tendons, especially the footprint—the most common region for tears.

All 97 patients underwent PUSB after the preliminary US examination (Fig. 3). The PUSB procedure is similar to a known technique (Cheng et al. 2015), but with modifications. First, the thickest and most superficial area of the subacromial–subdeltoid (SASD) bursa was located to determine the best injection site and approach (Fig. 4). Then, after sterilization of the skin over the target area, all patients were injected with subcutaneous lidocaine to anesthetize the local tissues and to ensure that the 22-G needle could reach the target area. Once the needle tip was visualized in the SASD bursa, contrast pulse sequencing was activated and 10–12 mL of contrast agent was gently injected into the SASD bursa under US guidance. We observed for leakage of contrast agent in real time during the injection and visualized its distribution again on video once we finished the CEUS examination.

Twenty-six patients underwent PUTL, which closely followed the PUSB procedure. The criteria for performing PUTL were (i) suspected lesion of the rotator cuff according to the preliminary US; and (ii) a confirmed intact superior surface of the cuff identified during PUSB, with evidence that the contrast agent was dispersed only in the bursa. The PUTL procedure was similar to the PUSB procedure, except that the contrast agent was injected into the area of the suspected tendon lesion directly (Fig. 4), and the average total volume of contrast agent used was 4–6 mL.

Both the PUSB and PUTL procedures took approximately 10 min. Dynamic contrast imaging data were recorded continuously during the procedures, which were stored for further analysis. The stored CEUS

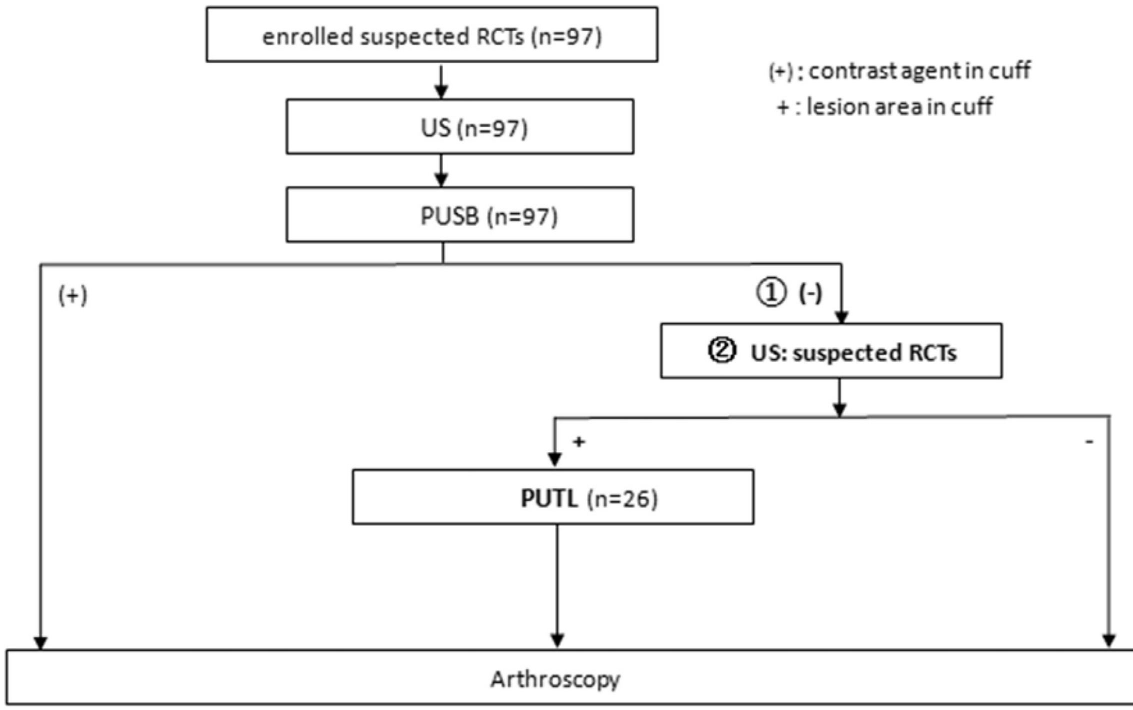

Fig. 3. Operative flowchart for US, PUSB and PUTL procedures in the detection of RCT subtypes. PUSB = percutaneous ultrasound-guided subacromial bursography; PUTL = percutaneous ultrasound-guided tendon lesionography; RCT = rotator cuff tear; US = ultrasound.

imaging data were reviewed again 30 min after the CEUS procedure (Cheng et al. 2015).

Image analysis. Two experienced sonographers with 12 and 8 y of experience in reading musculoskeletal US and with 9 and 6 y of experience in CEUS read all the images independently.

US

A full-thickness tear was diagnosed in cases of (i) non-visualization of the cuff because of massive full-thickness tears and retraction under the acromion; (ii) a localized defect area involving both the bursal and articular sides of the tendon on short- and long-axis views; and (iii) focal thinning and loss of continuity of the tendon. A partial-thickness tear was diagnosed when two perpendicular scans revealed (i) a distinct hypo-echoic defect or discontinuous region involving either the bursal or articular side of the tendon; (ii) a mixed hyper- and hypo-echoic area; and (iii) minimal flattening or concavity of a normally convex bursal-side surface of the cuff (a bursal-side partial-thickness tear) (Ellman 1990; Teefey et al. 2000; Jacobson et al. 2004).

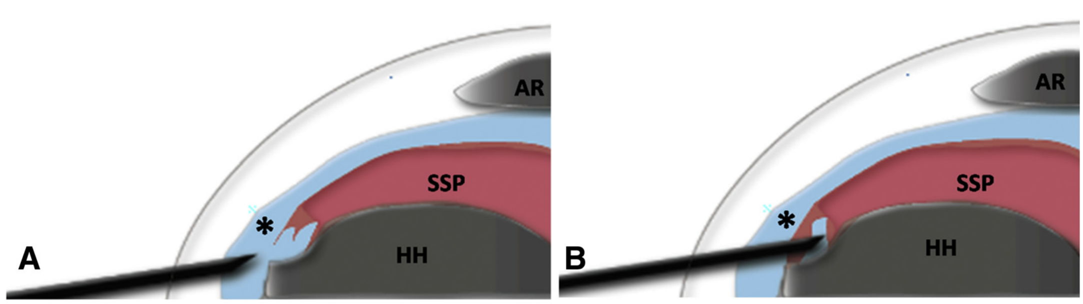

Fig. 4. Operative schematic of the PUSB and PUTL procedures. (A) Contrast agent was injected into the subacromial–subdeltoid bursa (*) during the PUSB procedure. (B) If contrast agent dispersed only within the bursa outlining the superior cuff surface and did not leak into the area of the lesion identified on ultrasound (US), PUTL would be performed with the needle tip injected into the lesion area directly. AR = acromion; HH = humeral head; PUSB = percutaneous ultrasound-guided subacromial bursography; PUTL = percutaneous ultrasound-guided tendon lesionography; SSP = supraspinatus.

Contrast-enhanced ultrasound

The distribution and localization of contrast agent (depth: SASD bursa, rotator cuff and/or glenohumeral joint cavity; width: larger or small) are key points for differentiating between larger or small full-thickness tears and bursal- or articular-side partial-thickness tears from an intact cuff.

A full-thickness tear was diagnosed when contrast agent either leaked from the bursa through the cuff and into the joint cavity during the PUSB procedure or extravasated from a cuff defect into both the bursa and joint cavity during the PUTL procedure. A bursal-side partial-thickness tear was identified when contrast agent either leaked from the bursa into solely the bursal-side cuff during the PUSB procedure or extravasated from a localized bursal-side cuff lesion into the bursa during the PUTL procedure. An articular-side partial-thickness tear could be detected only during the PUTL procedure, in which contrast agent appeared in the area of the cuff lesion, was limited to the articular-side tendon and flowed smoothly into the joint cavity. For an intact cuff, the contrast agent was dispersed solely within the bursa during the PUSB procedure and could not be injected into the tendon substance during the PUTL procedure.

Magnetic resonance imaging

Equipment. All MRI scans were performed on a 1.5-T scanner (Philips, Achieva, Netherlands) with a dedicated shoulder array coil. The field of view was 180 × 180 mm, the imaging matrix was 252 × 198 mm, the slice thickness/slice gap was 3 mm/0 mm and the number of excitations was 4. All patients had the following sequences performed: an oblique coronal T2-weighted imaging (T2-WI)−turbo spin echo (TSE) (TR = 4830 ms, TE = 100 ms); a transverse and oblique coronal T2-WI−short-time inversion recovery (STIR) (TR = 500 ms, TE = 18 ms); a transverse and oblique coronal T1-WI−TSE (TR = 500 ms, TE = 18 ms); and an oblique coronal proton density-weighted spectral adiabatic inversion recovery (PDW-SPAIR) (TR = 3959, TE = 30).

Image analysis. Two skilled radiologists, with 8 and 6 y of experience in musculoskeletal MRI, interpreted all images independently, and they were unfamiliar with US and CEUS results. A full-thickness tear was defined as involving the entire thickness of the cuff on the basis of the following imaging results: (i) an increased signal on the T2-weighted or PDW-SPAIR sequences and a loss of continuity on the T1-weighted sequences from the bursal to the articular side of the cuff; and (ii) a flat area or fluid-filled gap without visible fibers caused by retraction on all sequences. A partial-thickness tear was diagnosed when a localized thickness of the cuff was involved, that is, a focal discontinuity region on the T1-weighted sequences and an increased signal on the T2-weighted or PDW-SPAIR sequences in the corresponding area, only partially involving the cuff, either on the bursal or articular side of the tendon (Fukuda 2003; Rafii et al. 1990; Yamakawa et al. 2001).

Arthroscopy

Two senior orthopedic surgeons, with 12 and 18 y of experience in shoulder arthroscopy, performed all the arthroscopic examinations (including subacromial bursoscopy) and the operative procedures *via* the posterior portal. The presence or absence of the RCT subtypes were noted on arthroscopy. Criteria for the classification of partial- and full-thickness tears were based on Codman's and Cofield's classification systems, respectively (Codman 1934; Cofield 1985). In the present study, width of full-thickness tears >1 cm was defined as "larger."

Statistical analyses

Statistical analyses were performed using SPSS Version 13.0 (IBM, Armonk, NY, USA). US, MRI and CEUS findings were correlated with the prospective arthroscopy findings. Comparisons between the groups of tears and intact cuffs were made using the Mann−Whitney *U*-test or McNemar test. The data are expressed as the mean ± standard deviation, and the dichotomous variables are expressed as absolute frequencies and percentages. The rates of diagnosing RCT subtype *via* US, MRI and CEUS for larger full-thickness tears, small full-thickness tears, partial-thickness tears, small full-thickness tears combined with partial-thickness tears, bursal-side partial-thickness tears and articular-side partial-thickness tears were evaluated and compared using the χ^2-test ($\alpha = 0.05$, two-sided). The detection rates of the PUSB and PUTL procedures were evaluated and compared with those of US and MRI using the χ^2-test ($\alpha = 0.05$, two-sided) for full-thickness tears combined with bursal-side partial-thickness tears and all 26 cases in which PUTL was performed, respectively. Binary logistic regression analysis was performed to evaluate the role of confounding factors on goodness of fit between three imaging tests and arthroscopy, respectively. p Values < 0.05 were considered to indicate statistical significance.

Table 1. Population characteristics for all 97 cases

Arthroscopy (n = 97)	Tears (n = 72)	Intact cuffs (n = 25)	P Value*
Age (y)	49.3 ± 13.3	45.8 ± 13.1	0.283
Male (%)	48(67)	5 (60)	0.200
Trauma (%)	50 (69)	12 (48)	0.121
Course of disease (mo)	7.0 ± 5.3	9.8 ± 13.9	0.637

* Values of $p < 0.05$ indicate significance.

Table 2. US, MRI and CEUS findings in the detection of RCT subtypes

Arthroscopy	US					MRI					CEUS					Total
	lF	sF	bP	aP	NT	lF	sF	bP	aP	NT	lF	sF	bP	aP	NT	
lF	17	0	0	0	0	17	0	0	0	0	17	0	0	0	0	17
sF	0	10	0	4	0	0	10	0	4	0	0	14	0	0	0	14
bP	0	4	5	0	9	0	0	5	4	9	0	0	17	0	1	18
aP	0	3	2	18	0	0	2	0	19	2	0	0	0	23	0	23
No tear	0	2	1	0	22	0	0	2	0	23	0	0	2	0	23	25
Total	17	19	8	22	31	17	12	7	27	34	17	14	19	23	24	97

CEUS = contrast-enhanced ultrasound; MRI = magnetic resonance imaging; RCT = rotator cuff tear; US = ultrasound; lF = larger full-thickness tear; sF = small full-thickness tear; bP = bursal-side partial-thickness tear; aP = articular-side partial-thickness tear; NT = no tear.

RESULTS

Population characteristics and arthroscopic diagnoses in all 97 cases

There were no significant differences between the tear and intact cuff groups with respect to age, gender, history of trauma and course of disease (Table 1). Arthroscopy was performed on a total of 97 shoulders, and 17 larger full-thickness tears, 14 small full-thickness tears, 18 bursal-side partial-thickness tears, 23 articular-side partial-thickness tears and 25 intact rotator cuffs were identified (Table 2). All tears were surgically proved to be tears of the supraspinatus tendon except 17 that simultaneously involved the infraspinatus tendon. Among patients with intact cuffs, there were 2 with low elastic tendons (who had diabetes mellitus or hyperlipidemia), 2 with superior labrum anterior-to-posterior lesions, 9 with supraspinatus tendinopathy and 12 with SASD bursitis.

Comparison of CEUS, US and MRI in the detection of various RCT subtypes

The CEUS procedures were successfully performed with no severe complications, such as allergy and infection, during or after PUSB and PUTL. Patients only complained of slight pain when the needle penetrated the subcutaneous tissue during administration of the anesthetic.

A comparison of the diagnostic efficacy of US, MRI and CEUS with respect to detection of the various RCT subtypes is outlined in Table 3. The overall accuracies of US, MRI and CEUS were 74.2% (72/97), 76.3% (74/97) and 96.9% (94/97), respectively. Among 31 full-thickness tears, CEUS accurately detected all lesions, and US and MRI misinterpreted 4 small ones. Among the 18 bursal-side partial-thickness tears, 4 false-positive and 9 false-negative assessments were made on US, and 13 lesions were misdiagnosed on MRI as other types of tears or intact cuffs. There was only one false-negative case identified by CEUS. Considering the articular-side tears separately, 5 lesions were misdiagnosed on US as other types of tears. Two false-negative and 2 false-positive assessments were observed on MRI, whereas all 23 lesions were correctly identified with CEUS. Among the 25 intact cuffs, 3, 2 and 2 false-positive diagnoses were made on US, MRI and CEUS, respectively (Table 2). The detection rates with CEUS were significantly higher than those with US and MRI for the subtypes of tears, partial-thickness tears, combined small full-thickness and partial-thickness tears and bursal-side partial-thickness tears, respectively ($p < 0.001$) (Table 3). Of the 72 RCTs accurately detected on both US and CEUS, the tear contours were clearly outlined by the contrast agent, which provided better visualization with CEUS than US.

Table 3. Comparison of detection rates for US, MRI and CEUS in the diagnosis of the various RCT subtypes

	US (n/N)	MRI (n/N)	CEUS (n/N)	p (χ^2-test)
RCT subtypes	74.2% (72/97)	76.3% (74/97)	96.9% (94/97)	<0.001
lF	100.0% (17/17)	100.0% (17/17)	100.0% (17/17)	—
sF	71.4% (10/14)	71.4% (10/14)	100.0% (14/14)	0.085
PT	56.1% (23/41)	58.5% (24/41)	97.6% (40/41)	<0.001
sF + PT	60.0% (33/55)	61.8% (34/55)	98.2% (54/55)	<0.001
bP	27.8% (5/18)	27.8% (5/18)	94.4% (17/18)	<0.001
aP	78.3% (18/23)	82.6% (19/23)	100.0% (23/23)	0.068

CEUS = contrast-enhanced ultrasound; MRI = magnetic resonance imaging; US = ultrasound; lF = larger full-thickness tear; sF = small full-thickness tear; PT = partial-thickness tear; bP = bursal-side partial-thickness tear; aP = articular-side partial-thickness tear.

Table 4. Comparison of detection rates of US and MRI with that of PUSB in the detection of all 49 full-thickness and bursal-side partial-thickness tears, and with PUTL in the detection of all 26 patients who underwent the PUTL procedure

Method	US	MRI	PUSB^A / PUTL^B	p (χ^2-test)
A% (n_A/N_A)	65.3% (32/49)	65.3% (32/49)	93.9% (46/49)^A	0.001
B% (n_B/N_B)	69.2% (18/26)	76.9% (20/26)	100.0%(26/26)^B	0.011

MRI = magnetic resonance imaging; PUSB = percutaneous ultrasound-guided subacromial bursography; PUTL = percutaneous ultrasound-guided tendon lesionography; US = ultrasound; N_A, N_B = numbers of cases that could have been accurately detected by PUSB and PUTL, respectively.

Comparison of PUSB, US and MRI in detection of combined full-thickness and bursal-side partial-thickness tears

Among all full-thickness and bursal-side partial-thickness tears, PUSB accurately detected 46 of 49 (93.9%) lesions. The detection accuracy was significantly higher than that of US and MRI ($p = 0.001$) (Table 4). Three false-negative and 2 false-positive assessments occurred with PUSB.

Comparison of PUTL, US and MRI in detection of all 26 lesions after PUTL procedure

Only the cuffs that were suspected of being torn that were not detected on PUSB needed to undergo the PUTL procedure. Therefore, PUTL was performed in 26 cases, including 2 small full-thickness tears missed as intact tendons on PUSB and misdiagnosed as articular-side partial-thickness tears on US. One intact cuff was identified as having no tear on PUSB, but was misdiagnosed as having a bursal-side partial-thickness tear on US. Twenty-three articular-side partial-thickness tears had suspected lesions on US but no tears were identified on PUSB. Overall, PUTL accurately diagnosed all 26 lesions, including 2 that were misdiagnosed on PUSB and 8 that were misinterpreted on US. The accuracy of PUTL (100.0%) was significantly higher than that of US (69.2%) and MRI (76.9%) in diagnosing the 26 lesions ($p = 0.011$) (Table 4).

DISCUSSION

Rotator cuff tears are a common cause of shoulder pain and dysfunction. The indications for operative treatment of RCTs have not been sufficiently defined (Lenza et al. 2013). Although many factors are associated with healing outcomes among arthroscopically repaired cuffs, some studies have indicated that the tear size has an association with the final post-operative result and that partial- or small full-thickness tears often have satisfactory surgical outcomes (Bianchi 2005; Bryant 2002; Cho and Rhee 2009; Fotiadou 2008; Lenza et al. 2013). Currently, neither US nor MRI is the definitely accepted method of choice in diagnosing RCT subtypes (Swen et al. 1999). US echogenicity lacks specificity, and MRI could not effectively detect partial- and small full-thickness tears (Ellman 1990). Therefore, we aimed to explore the reliability and efficacy of CEUS as an alternative method in the diagnosis of RCT subtypes. Overall, we found that CEUS, a combination of PUSB and PUTL, is effective in detecting RCT subtypes with relatively higher accuracy than US and MRI. This technique can reliably identify, localize and determine the extent of RCTs, which is beneficial for clinical management.

In the present study, the overall accuracies of US and MRI were 74.2% and 76.3%, respectively, in the detection of RCT subtypes. US (56.1%) and MRI (58.5%) had poor accuracy in the detection of partial-thickness tears, the accuracies of which were even lower than reported in earlier studies (Martín-Hervás et al. 2001; Milosavljevic et al. 2005; Teefey et al. 2000, 2004), although they had equally high accuracies in the detection of full-thickness tears. This may be because the previously reported studies focused on the broader classification scheme for RCTs, including full- or partial-thickness tears only, not the subtypes. In this study, CEUS enhanced the marginal contrast of the torn area within the tendons, which allowed ultrasonographic identification of RCTs in a significantly larger proportion of cases with an overall accuracy of 96.9% for the subtypes and 97.6% for partial-thickness tears. Overall, our results support the role of CEUS as an effective alternative imaging technique in the diagnosis of RCT subtypes. Our findings indicated that CEUS performed better than US and MRI, especially in the assessment of small full-thickness and partial-thickness tears.

The initial purpose of this investigation was to determine whether PUSB could enhance the efficacy of identifying full-thickness and bursal-side partial-thickness tears.

Theoretically, PUSB should be superior to US in diagnosing full-thickness and bursal-side partial-thickness tears. The present study found that the detection rates were 65.3% for both US and MRI, but 93.9% for PUSB, which was slightly higher than the previously reported 92.1% (Cheng et al. 2015). The reason may be that Cheng et al. (2015) evaluated all lesions, including those with articular partial-thickness tears that could not be confirmed on PUSB. In practice, PUSB correctly assessed 14 lesions more than US and MRI, including 2 small full-thickness tears and 12 bursal-side partial-thickness tears.

The 2 small full-thickness tears were misdiagnosed as large articular-side partial-thickness tears on US, because of confounding of the irregular proliferative synovium over the bursal-side cuff, which was confirmed surgically. With respect to full-thickness tears, non-visualization or focal discontinuity of the tendon is the best imaging sign to confirm the diagnosis. Among small full-thickness tears, focal abnormal echogenicity is sometimes the only sign; however, it lacks specificity because it can be present in cases of partial-thickness tears, tendinitis, surgical scars and even degenerated but intact cuffs (Ellman 1990). Middleton et al. (2004) reported that for two experienced observers, the primary cause of inter-observer variability was related to the difficulty in distinguishing extensive partial-thickness tears from full-thickness tears.

In our study, the majority of misdiagnoses on US and MRI occurred with bursal-side partial-thickness tears. The detection rates were 27.8% (5/18) for both US and MRI, which were extremely lower than those in previous reports (Chun et al. 2010; Fotiadou 2008). Among the subtypes of partial-thickness tears, the incidence of the bursal-side subtype in our study was almost equal to that of the articular-side subtype, which was much higher than the incidence reported in previously published series (Chun et al. 2010; McConville and Ianotti 1999; Olsewski and Depew 1994). This may be due to an underestimation of the accuracy of US and MRI in the detection of partial-thickness tears. Among the 13 misinterpreted bursal-side partial-thickness tears, there were 4 large bursal-side partial-thickness tears that were misinterpreted as small full-thickness tears on conventional US, with only the existing membrane-like structure on the articular side of the cuff confirmed *via* arthroscopy (Fig. 5; Supplementary Video S1, online only). Other researchers (Teefey et al. 2000, 2004) have reported that large partial-thickness tears may mimic full-thickness tears on ultrasound because of their compressibility and can be easily misinterpreted. The remaining 9 lesions were misdiagnosed as intact cuffs because the comparatively small and atypical lesions were difficult to differentiate on conventional US and MRI. Ellman (1990) reported that negative imaging results could not always be presumed to be intact cuffs may ultimately be confirmed to be one of a variety of partial-thickness tears at the time of surgery.

A second purpose of this study was to evaluate whether PUTL is a tolerable modality and increases the detection rate in the differentiation of RCT subtypes.

Although PUSB is relatively superior to US and MRI because it reveals more visible and objective US features of RCTs, it could not detect all subtypes of

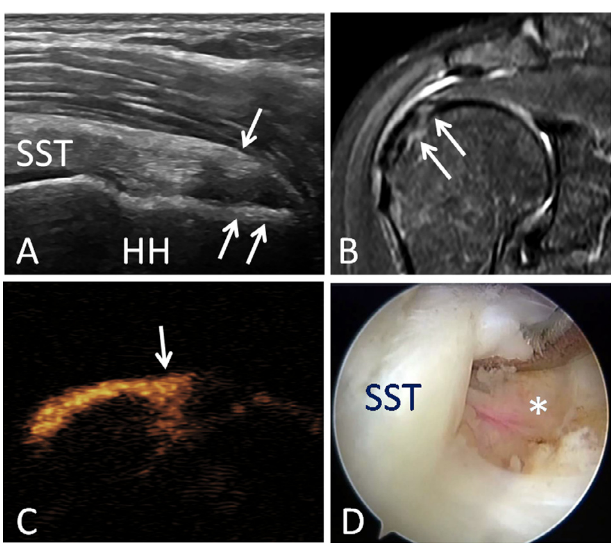

Fig. 5. Large bursal-side partial-thickness tear in a 51-y-old woman. (A) Ultrasound revealed a local defect area with an extension through both the articular and bursal surfaces of the supraspinatus tendon (↑↑) and hyper-echoic peribursal fat filling a small superficial defect (↑) in the long-axis view. (B) An oblique coronal T2-weighted image revealed a brighter signal on the articular side of the involved tendon (↑↑). (C) Percutaneous ultrasound-guided subacromial bursography image revealed contrast agent filling and outlining the torn tendon (↑) located only at the bursal-side cuff in the long-axis view. (D) Arthroscopy confirmed a large bursal-side partial-thickness tear with only a membrane-like residual on the articular side (*). HH = humeral head; SST = supraspinatus tendon.

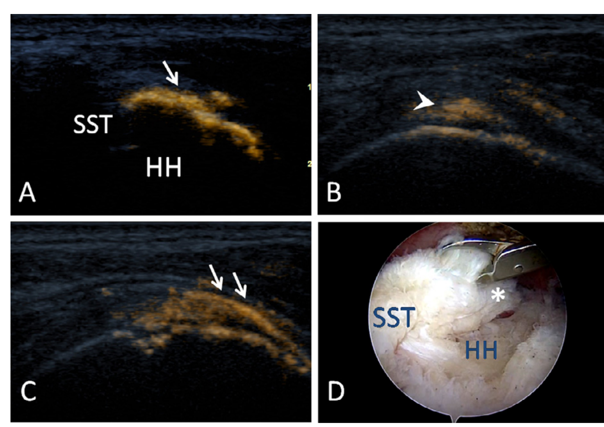

Fig. 6. Small full-thickness tear in a 56-y-old woman. (A) Percutaneous ultrasound-guided subacromial bursography image revealed that hyper-echoic contrast agent was dispersed only within the bursa outlining an irregular superior bursal cuff surface (↑); it did not leak into the tendon in the long-axis view. (B) Percutaneous ultrasound-guided tendon lesionography image revealed that hyper-echoic contrast agent was localized within the tendon (*arrowhead*) in the long-axis view. (C) As the amount increased, the contrast agent filled and outlined the tear area, then leaked into the glenohumeral joint cavity and finally into the irregular bursa (↑↑) in the long-axis view. (D) Arthroscopy confirmed a small full-thickness tear (*) with severe synovial proliferation on the bursal-side cuff. HH = humeral head; SST = supraspinatus tendon.

RCTs. Thus, the present study advanced the concept of PUTL to make up for the deficiency of PUSB. The contrast agent used in this work was SonoVue, which was reported to be tolerable in clinical practice and previously published research (Cheng et al. 2015; Lee et al. 2014). After PUSB, arthrosonography was not used as the first choice because of the difficulty of puncture and the dosage of contrast agent; however, PUTL was used after PUSB. Concerns that PUTL would extend beyond the area of the lesion associated with the contrast agent injection are unfounded. In practice, it is difficult to inject contrast agent into an intact tendon because of its high density. Additionally, during PUTL, we depressed the syringe very gently so that the contrast agent would appear only within the area of the defect. Lower dosages of contrast agent administered during PUTL resulted in lower tension to the torn area.

Theoretically, PUTL can detect any RCT subtype. In practice, this procedure facilitated accurate assessments of all 26 patients who underwent the procedure. PUTL correctly diagnosed 2 small full-thickness tears that were misinterpreted on US, MRI and even PUSB (Fig. 6). These discrepancies may be attributed to the small irregular bursal-side tear area and the proliferative synovium over the bursal side of the cuff, which prevented smooth contrast agent flow into the tear area from the bursa. Contrast agent might more easily leak into the bursa from the tear regions in the tendon during the PUTL procedure. Thus, in everyday practice we should pay close attention to abnormal ultrasonogram appearances of the bursal side of the tendon. PUTL correctly diagnosed all 23 articular-side partial-thickness tears (Fig. 7; Supplementary Video S2, online only), whereas 5 and 4 of them were misdiagnosed on US and MRI, respectively. Among the misdiagnosed cases, 2 were overestimated to be small full-thickness tears on both US and MRI. The causes of the misdiagnoses were also attributed to the difficulty in distinguishing extensive partial- from full-thickness tears (Teefey et al. 2000). Two of the tears were misdiagnosed as bursal-side partial-thickness tears on US, and no tears were seen on MRI. The causes of the errors were multifactorial, with the chronic nature of the tears possibly playing a vital role in the misdiagnosis, especially among unexperienced radiologists (Middleton et al. 2004). The investigators suggested that extensive tears of the tendon with effusion could be easily visualized, whereas chronic tears without effusion and with heterogeneous features on US might mimic tendinopathy (Teefey et al. 2004). However, contrast agent easily diffused into the areas of the lesion, delineating the location and extent of the tear area well and producing hyper-echoic lines that strongly increased the echogenicity of the tendon fiber texture. PUTL accurately depicted intact tendons confirmed to be severe bursitis arthroscopically that were misidentified as bursal-side partial-thickness tears on US (Supplementary Video S3, online only). A possible cause might also be the extremely irregular proliferative synovium of SASD, which was difficult to identify on conventional US.

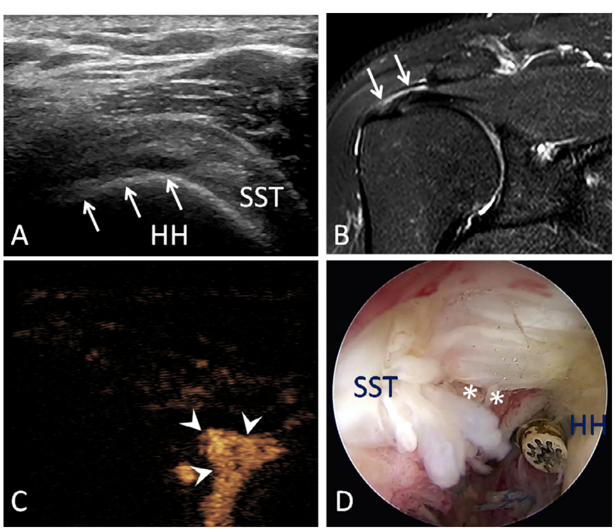

Fig. 7. Articular-side partial-thickness tear in a 35-y-old man. (A) Ultrasound image revealed a hypo-echoic area with unclear bursal-side margin on the articular side of the tendon (↑↑↑), which was shown on ultrasound (US) imaging in a long-axis view. There seemed to be a small articular-side partial-thickness tear with about 30% of the cuff thickness involved. (B) Oblique coronal T2-weighted image revealed a brighter signal on the bursal side of the involved tendon (↑↑). (C) Percutaneous ultrasound-guided tendon lesionography image revealed contrast agent filling in the tear area of the articular side more clearly, and leaking into the glenohumeral joint cavity in real time (*arrowhead*), which indicated a large articular-side partial-thickness tear in the long-axis view. (D) Arthroscopy confirmed a large articular-side partial-thickness tear (**). HH = humeral head; SST = supraspinatus tendon.

Among all 97 cases, CEUS misinterpreted 3 lesions, including 2 atypical intact cuffs overestimated to be bursal-side partial-thickness tears on PUSB, and one bursal-side partial-thickness tear that was missed on PUSB. Arthroscopy revealed that the 2 atypical intact cuffs were minimally elastic, which may be inherently correlated with cuff texture. One of the patients was a diabetic (Fig. 8), and another had severe hyperlipidemia, both for about 10 y. There was some contrast agent leakage into the cuff, but not into the joint cavity, during the PUSB procedures. The two cases were misdiagnosed on US and MRI. Either diabetes or hyperlipidemia is one of the independent risk factors for the development of RCTs (Lin et al. 2015). One reason hyperglycemia increases the risk of RCTs is that the excessive accumulation of advanced glycation end-metabolism products (DeGroot 2004; Dutta et al. 2007) can make the tendon weaker, less elastic and more susceptible to tearing by

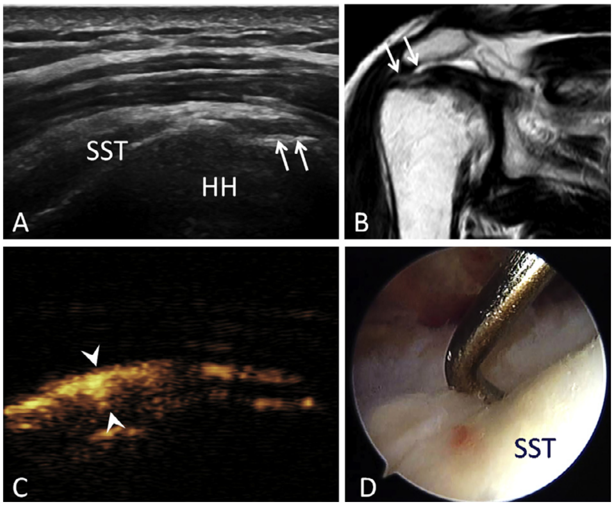

Fig. 8. Intact rotator cuff in a 33-y-old male diabetic. (A) Ultrasound revealed a focal hypo-echoic tendon, but could not differentiate the bursal-side partial-thickness tear from the full-thickness tear (↑↑) in the long-axis view. (B) An oblique coronal T2-weighted image revealed a brighter signal on the bursal side of the involved tendon (↑↑) that appeared to be consistent with poor elasticity. (C) Percutaneous ultrasound-guided subacromial bursography image revealed contrast agent filling and outlining the tear area of the bursal-side tendon (*arrowhead*). Thus, the lesion was misdiagnosed as a bursal-side partial-thickness tear in the long-axis view. (D) Arthroscopy confirmed a stiffer, less elastic tendon with no tear. HH = humeral head; SST = supraspinatus tendon.

changing the physicochemical properties of the proteins (Abate et al. 2010; Ippolito et al. 1980). Hyperlipidemia can cause fatty infiltration effects because of lipid deposition in tendon, which can make tendon tear easily and make repairs difficult (Chaudhury et al. 2012; Kannus et al. 2005). Therefore, before performing the RCT examination, we should be alerted to any history of diabetes and hyperlipidemia, in addition to taking the patient's age and history of injury into account. Another misinterpreted lesion was a small bursal-side partial-thickness tear that was suspected to be a tendinopathy because no lesion was visualized on US, and the lesion was thought to be an intact tendon on PUSB. As such, this patient did not undergo a PUTL procedure.

The present study has some limitations. First, the techniques are invasive with well-recognized risks, such as infection, despite our lack of complications. Another possible limitation of the study is that surgeons were not blinded to the results of imaging tests for benefit of patients, which may cause a bias in surgical decisions and further influences patient selection. Also, some confounders may have influenced the goodness of fit for US and MRI compared with arthroscopy. Decreased degrees of tear extent increase the misdiagnosis rate for both US and MRI, which is the purpose of our study with respect to identifying improved ultrasound techniques. Other confounder was age in the case of MRI. It is possible that the age-related degeneration made differentiating tendinopathy from small partial-thickness tears on MRI more difficult because the majority of the misdiagnosed cases occurred in patients who were older than 50 y. None of the five possible confounders—age, gender, trauma, course of disease and tear extent—significantly influenced the goodness of fit between CEUS and arthroscopy. However, a prospective study with a large patient study population should be carried out to further analyze the specific impacts of these confounders. Furthermore, as a preliminary report, we only explored the feasibility and effectiveness of CEUS. In future studies, we will further explore and intend to identify optimal methods for defining a standard clinical algorithm for diagnosis and management, especially for symptomatic partial-thickness tears.

CONCLUSIONS

This preliminary prospective report described the feasibility and effectiveness of PUTL, an imaging modality using SonoVue. CEUS, a combination of PUSB and PUTL, represents an effective alternative method for detecting subtypes of RCTs with relatively higher accuracy than with US and MRI. This technique can reliably identify and localize the extent of RCTs, which is beneficial for clinical management.

Acknowledgments—This study received funding from Tianhe Science and Technology Project 201604 KW031, Guangzhou, Guangdong, China; Guangdong Science and Technology Project 2014 A020212169, China; and National Natural Science Foundation of China 81771853. The first organisation provided financial support for the study design, collection, analysis and interpretation of data, the writing of the report and the decision to submit the article for publication. The latter two organizations provided financial support for the decision to submit the article for publication. We gratefully acknowledge the foundations for their grants-in-aid, the ethics committee of our hospital for approving the study and the efforts of Ying Guan's team, from the Epidemiology Research Unit, Southern Medical University, for their invaluable help with the statistical analyses

SUPPLEMENTARY MATERIALS

Supplementary material associated with this article can be found in the online version at doi:10.1016/j.ultrasmedbio.2018.10.012.

REFERENCES

Abate M, Schiavone C, Salini V. Sonographic evaluation of the shoulder in asymptomatic elderly patients with diabetes. BMC Musculoskelet Disord 2010;11:278.

Bertuglia A, Mollo G, Bullone M, Riccio B. Identification of surgically-induced longitudinal lesions of the equine deep digital flexor tendon in the digital flexor tendon sheath using contrast-enhanced ultrasonography: An *ex vivo* pilot study. Acta Vet Scand 2014;56:78.

Bianchi S, Martinoli C, Abdelwahab IF. Ultrasound of tendon tears: Part 1. General considerations and upper extremity. Skeletal Radiol 2005;34:500–512.
Brooks CH, Revell WJ, Heatley FW. A quantitative histological study of the vascularity of the rotator cuff tendon. J Bone Joint Surg Br 1992;74:151–153.
Bryant L, Shnier R, Bryant C, Murrell GA. A comparison of clinical estimation, ultrasonography, magnetic resonance imaging, and arthroscopy in determining the size of rotator cuff tears. J Shoulder Elbow Surg 2002;11:219–224.
Chaudhury S, Dines JS, Delos D, Warren RF, Voigt C, Rodeo SA. Role of fatty infiltration in the pathophysiology and outcomes of rotator cuff tears. Arthritis Care Res 2012;64:76–82.
Cheng X, Lu M, Yang X, Guo X, He F, Chen Q, Gu P. The effect of percutaneous ultrasound-guided subacromial bursography using microbubbles in the assessment of subacromial impingement syndrome: Initial experience. Eur Radiol 2015;25:2412–2418.
Cho NS, Rhee YG. The factors affecting the clinical outcome and integrity of arthroscopically repaired rotator cuff tears of the shoulder. Clin Orthop Surg 2009;1:96–104.
Choo HJ, Lee SJ, Kim JH, Kim DW, Park YM, Kim OH, Kim SJ. Delaminated tears of the rotator cuff: Prevalence, characteristics, and diagnostic accuracy using indirect MR arthrography. AJR Am J Roentgenol 2015;204:360–366.
Chun KA, Kim MS, Kim YJ. Comparisons of the various partial-thickness rotator cuff tears on MR arthrography and arthroscopic correlation. Korean J Radiol 2010;11:528–535.
Codman EA, editor. The shoulder. Boston: Thomas Todd; 1934.
Cofield RH. Rotator cuff disease of the shoulder. J Bone Joint Surg Am 1985;67:974–979.
Daenen B, Houben G, Bauduin E, Lu KV, Meulemans JL. Ultrasound of the shoulder. JBR-BTR 2007;90:325–337.
DeGroot J. The AGE of the matrix: Chemistry, consequence and cure. Curr Opin Pharmacol 2004;4:301–305.
Donohue NK, Nickel BT, Grindel SI. High-grade articular, bursal, and intratendinous partial-thickness rotator cuff tears: A retrospective study comparing functional outcomes after completion and repair. Am J Orthop 2016;45:E254–E260.
Dutta U, Cohenford MA, Guha M, Dain JA. Non-enzymatic interactions of glyoxylate with lysine, arginine, and glucosamine: A study of advanced non-enzymatic glycation like compounds. Bioorg Chem 2007;35:11–24.
Ellman H. Diagnosis and treatment of incomplete rotator cuff tears. Clin Orthop Relat Res 1990;254:64–74.
Fotiadou AN, Vlychou M, Papadopoulos P, Karataglis DS, Palladas P, Fezoulidis IV. Ultrasonography of symptomatic rotator cuff tears compared with MR imaging and surgery. Eur J Radiol 2008;68:174–179.
Franceschi F, Papalia R, Palumbo A, Del Buono A, Maffulli N, Denaro V. Operative management of partial- and full-thickness rotator cuff tears. Med Sport Sci 2012;57:100–113.
Fukuda H. Partial-thickness rotator cuff tears: A modern view on Codman's classic. J Shoulder Elbow Surg 2000;9:163–168.
Fukuda H. The management of partial-thickness tears of the rotator cuff. J Bone Joint Surg 2003;85:3–11.
Fukuda H, Hamada K, Nakajima T, Yamada N, Tomonaga A, Goto M. Partial-thickness tears of the rotator cuff: A clinicopathological review based on 66 surgically verified cases. Int Orthop 1996;20:257–265.
Gladstone JN, Bishop JY, Lo IK, Flatow EL. Fatty infiltration and atrophy of the rotator cuff do not improve after rotator cuff repair and correlate with poor functional outcome. Am J Sports Med 2007;35:719–728.
González RR. Direct magnetic resonance arthrography, indirect magnetic resonance arthrography, and computed tomography arthrography for rotator cuff lesions and superior labral anterior and posterior tears: State of the art? Radiología 2013;55:283–293.
Hanchard NC, Lenza M, Handoll HH, Takwoingi Y. Physical tests for shoulder impingements and local lesions of bursa, tendon or labrum that may accompany impingement. Cochrane Database Syst Rev 2013;4:CD007427.
Hodler J, Kursunoglu-Brahme S, Snyder SJ, Cervilla V, Karzel RP, Schweitzer ME, Flannigan BD, Resnick D. Rotator cuff disease: Assessment with MR arthrography versus standard MR imaging in 36 patients with arthroscopic confirmation. Radiology 1992;182:431–436.
Ippolito E, Natali PG, Postacchini F, Accinni L, De Martino C. Morphologic, immunochemical, and biochemical study of rabbit Achilles tendon at various ages. J Bone Joint Surg Am 1980;62:583–598.
Jacobson JA, Lancaster S, Prasad A, van Holsbeeck MT, Craig JG, Kolowich P. Full-thickness and partial-thickness supraspinatus tendon tears: Value of US signs in diagnosis. Radiology 2004; 230:234–242.
Jain NB, Luz J, Higgins LD, Dong Y, Warner JJ, Matzkin E, Katz JN. The diagnostic accuracy of special tests for rotator cuff tear: The ROW cohort study. Am J Phys Med Rehabil 2017;96:176–183.
Kannus P, Paavola M, Jozsa L. Aging and degeneration of tendons. In: Maffulli N, Renstrom P, Leadbetter W, (eds). Tendon injuries: Basic science and clinical medicine. London: Springer-Verlag; 2005. p. 25–31.
Kim HM, Dahiya N, Teefey SA, Keener JD, Galatz LM, Yamaguchi K. Relationship of tear size and location to fatty degeneration of the rotator cuff. J Bone Joint Surg Am 2010;92:829–839.
Lee KW, Yang DS, Chun TJ, Bae KW, Choy WS, Park HJ. A comparison of conventional ultrasonography and arthrosonography in the assessment of cuff integrity after rotator cuff repair. Clin Orthop Surg 2014;6:336–342.
Lenza M, Buchbinder R, Takwoingi Y, Johnston RV, Hanchard NC, Faloppa F. Magnetic resonance imaging, magnetic resonance arthrography and ultrasonography for assessing rotator cuff tears in people with shoulder pain for whom surgery is being considered. Cochrane Database Syst Rev 2013;9:CD009020.
Lin TT, Lin CH, Chang CL, Chi CH, Chang ST, Sheu WH. The effect of diabetes, hyperlipidemia, and statins on the development of rotator cuff disease. Am J Sports Med 2015;43:2126–2132.
Martín-Hervás C, Romero J, Navas-Acién A, Reboiras JJ, Munuera L. Ultrasonographic and magnetic resonance images of rotator cuff lesions compared with arthroscopy or open surgery findings. J Shoulder Elbow Surg 2001;10:410–415.
Massoud SN, Levy O, Copeland SA. Subacromial decompression: Treatment for small-and medium-sized tears of the rotator cuff. J Bone Joint Surg Br 2002;84:955–960.
McConville OR, Ianotti JP. Partial-thickness tears of the rotator cuff: Evaluation and management. J Am Acad Orthop Surg 1999;7:32–43.
Meister K, Thesing J, Montgomery MJ, Indelicato PA, Walczak S, Fontenot W. MR arthrography of partial thickness tears of the undersurface of the rotator cuff: An arthroscopic correlation. Skeletal Radiol 2004;33:136–141.
Middleton WD, Teefey SA, Yamaguchi K. Sonography of the rotator cuff: Analysis of inter-observer variability. AJR Am J Roentgenol 2004;183:1465–1468.
Milosavljevic J, Elvin A, Rahme H. Ultrasonography of the rotator cuff: A comparison with arthroscopy in one-hundred-and-ninety consecutive cases. Acta Radiol 2005;46:858–865.
Mitchell C, Adebajo A, Hay E, Carr A. Shoulder pain: Diagnosis and management in primary care. BMJ 2005;331:1124–1128.
Olsewski JM, Depew AD. Arthroscopic subacromial decompression and rotator cuff debridement for stage II and stage III impingement. Arthroscopy 1994;10:61–68.
Probyn LJ, White LM, Salonen DC, Tomlinson G, Boynton EL. Recurrent symptoms after shoulder instability repair: Direct MR arthrographic assessment correlation with second-look surgical evaluation. Radiology 2007;245:814–823.
Rafii M, Firooznia H, Sherman O, Minkoff J, Weinreb J, Golimbu C, Gidumal R, Schinella R, Zaslav K. Rotator cuff lesions: Signal patterns at MR imaging. Radiology 1990;177:817–823.
Reilly P, Macleod I, Macfarlane R, Windley J, Emery RJ. Dead men and radiologists don't lie: A review of cadaveric and radiologic studies of rotator cuff tear prevalence. Ann R Coll Surg Engl 2006;88:116–121.
Resnick D, Kang HS, Pretter Klieber ML. Shoulder. In: Resnick D, Kang HS, Pretter Klieber ML, (eds). Internal derangements of joints. 2nd ed.Philadelphia, PA: Elsevier; 2007.

Rutten MJ, Spaargaren GJ, van Loon T, Kiemeney LA, Jager GJ. Detection of rotator cuff tears: The value of MRI following ultrasound. Eur Radiol 2010;20:450–457.
Safran O, Schroeder J, Bloom R, Weil Y, Milgrom C. Natural history of nonoperatively treated symptomatic rotator cuff tears in patients 60 y old or younger. Am J Sports Med 2011;39:710–714.
Singisetti K, Hinsche A. Shoulder ultrasonography versus arthroscopy for the detection of rotator cuff tears: Analysis of errors. J Orthop Surg (Hong Kong) 2011;19:76–79.
Song KD, Kwon JW, Yoon YC, Choi SH. Indirect MR arthrographic findings of adhesive capsulitis. AJR Am J Roentgenol 2011;197: W1105–W1109.
Swen WA, Jacobs JW, Algra PR, Manoliu RA, Rijkmans J, Willems WJ, Bijlsma JW. Sonography and magnetic resonance imaging equivalent for the assessment of full-thickness rotator cuff tears. Arthritis Rheum 1999;42:2231–2238.
Tashjian RZ. Epidemiology, natural history, and indications for treatment of rotator cuff tears. Clin Sports Med 2012;31: 589–604.
Teefey SA, Hasan SA, Middleton WD, Patel M, Wright RW, Yamaguchi K. Ultrasonography of the rotator cuff: A comparison of ultrasonographic and arthroscopic findings in one hundred consecutive cases. J Bone Joint Surg Am 2000;82:498–504.
Teefey SA, Rubin DA, Middleton WD, Hildebolt CF, Leibold RA, Yamaguchi K. Detection and quantification of rotator cuff tears: Comparison of ultrasonographic, magnetic resonance imaging, and arthroscopic findings in seventy-one consecutive cases. J Bone Joint Surg (Am) 2004;86:708–716.
Urwin M, Symmons D, Allison T, Brammah T, Busby H, Roxby M, Simmons A, Williams G. Estimating the burden of musculoskeletal disorders in the community: The comparative prevalence of symptoms at different anatomic sites, and the relation to social deprivation. Ann Rheum Dis 1998;57:649–655.
van Kampen DA, van den Berg T, van der Woude HJ, Castelein RM, Scholtes VA, Terwee CB, Willems WJ. The diagnostic value of the combination of patient characteristics, history, and clinical shoulder tests for the diagnosis of rotator cuff tear. J Orthop Surg Res 2014;9:70.
Wright SA, Cofield RH. Management of partial-thickness rotator cuff tears. J Shoulder Elbow Surg 1996;5:458–466.
Yagci B, Manisali M, Yilmaz E, Ozkan M, Ekin A, Ozaksoy D, Kovanlikaya I. Indirect MR arthrography of the shoulder in detection of rotator cuff ruptures. Eur Radiol 2001;11:258–262.
Yamakawa S, Hashizume H, Ichikawa N, Itadera E, Inoue H. Comparative studies of MRI and operative findings in rotator cuff tear. Acta Med Okayama 2001;55:261–268.